SI Appendix (Russo et al.)

Materials and Methods

Cell Culture

Primary mouse keratinocytes were isolated from newborn skin as described (1) and cultured under low calcium condition (0.05mM) in 4% calcium-chelated Fetal Bovine Serum (FBS) (Thermo Fisher Scientific) and Epidermal Growth Factor (EGF) (Thermo Fisher Scientific). Neonatal HDFn (Thermo Fisher Scientific), HEK293, H1299 and Saos-2 were grown in Dulbecco's Modified Eagle Medium (DMEM) and 10% FBS (Thermo Fisher Scientific).

Plasmids, transfections and luciferase assay

All *p63* mutant constructs were obtained using the QuikChange site-directed mutagenesis kit (Agilent) starting from either pCMV2-FLAG-mΔNp63α or pcDNA3.1-Myc-hΔNp63α using mutagenesis primers (Table S4). For HDF to iKC conversion, wild type p63 and its mutants were cloned in pBABE in the BamHI site. Cells were transfected using Lipofectamine 2000 (Thermo Fisher Scientific). Luciferase activity was determined 48 hr after transfection using the dual-luciferase reporter assay kit (Promega). pKRT14 promoter-luc (2), pG13-luc (3), and pFGFR2 enhancer-luc (1) were used as reporters. Renilla activity was used to normalize transfection efficiency. For *E. coli* expression of the murine wild-type and mutant p63 SAM domains see Supplementary Information.

Adenoviral infection and retroviral infection

Mouse primary keratinocytes were infected 5 days after plating with adenovirus carrying GFP as control or Cre recombinase at MOI 100 for 2 hr in low calcium medium without serum and EGF. Cells were collected four days after infection. High titer retroviral production was obtained in HEK293T cells by transient transfection of the pBABE constructs and of amphotropic viral envelope plasmid (pAmpho) using Lipofectamine 2000 (Thermo Fisher Scientific) as described (4). Cell supernatants containing the retroviruses were collected 48 and 72 hr after transfection. Neonatal HDF were infected twice at 20-30% confluence with retroviruses carrying p63 and KLF4 (5) in the presence of 8 μg/ml Polybrene. Cells were passage, selected with 2 μg/ml puromycin 48 hr after the second infections, and grown after 48 hr of selection for 15-18 days in the absence of puromycin as previously described (6).

Generation of the L514F conditional knock-in construct

A genomic portion of the mouse *p63* gene (16265bp) from exon 12 to the 3'UTR derived from the bMQ-241L2 BAC clone was subcloned into NotI and SpeI restriction site of pL253 vector via gap repair (7). Miniarms were cloned into the NotI and SpeI sites of pL253 using Ap63CDNU and Ap63CDNL, or Bp63CDNU and Bp63CDNL oligonucleotide primers. The PCR products were digested with NotI and HindIII (Ap63CDNU/L), or HindIII and SpeI (Bp63CDNU/L) respectively. The vector was subsequently linearized with HindIII and electroporated into the recombinogenic bacterial strain EL350 containing the bMQ-241L2 BAC clone to obtain the pL253-p63 plasmid. To insert a first LoxP site 400bp upstream of exon 13, miniarms (PCR product: CmP63U-CmP63L and DmP63U-DmP63L) were cloned into NotI-EcoRI or BamHI-SalI sites in the pL452 vector (7) containing the PGK-Neo cassette flanked by LoxP sites. The "armed" PGK-Neo cassette and pL253-P63 were co-electroporated into the recombinogenic bacterial strain EL350. PGK-Neo cassette was excised by Cre-recombinase to obtain pL253-P63Lox1 plasmid. Two unique restriction enzyme sites (ISceI and ICeuI) flanking Blasticidin (Bsd) were inserted in the pL253-p63Lox1 plasmid to substitute exon 14. Miniarms (PCR product: C1mP63U-C1mP63L and D1mP63U-D1mP63L) were cloned into NotI-

EcoRI or BamHI-SalI sites in the the pBS I-SceI-Bsd-I-CeuI vector. The "armed" I-SceI-Bsd-I-CeuI cassette was co-electroporated with the pL253-P63Lox1 plasmid into the bacterial strain EL350 to obtain the pL253-P63Lox1-Bsd plasmid.

To insert 3xFlag tag in the p63 exon 14, genomic DNA was amplified with P63ex14fgU-P63ex14fgL, and the PCR product was digested with EcoRI and SmaI to insert in BamHI (filled) - KpnI sites of p3xFlag-CMV-14-C (Sigma). p63 exon 14 -3xFlag was amplified from p3xFlag-CMV-p63ex14 using ISceIE14U and ICeuIFlagL oligonucleotides and cloned into ISceI and ICeuI restriction sites of pL253-P63Lox1-Bsd to generate pL253-P63Lox1-Ex14-3xFlag.

Subsequently, genomic DNA was amplified with DmP63U2, Ex13L2 oligonucleotides and cDNA with Ex13U2, RecEx14L3 oligonucleotides to generate a DNA fragment containing p63 exons 13 and 14 fused by recombinant PCR. At the same time, mutant p63 exon 13 (L514F) was generated by recombinant PCR using DmP63U, Ex13MutL, Ex13MutU, RecEx13L oligonucleotides. These 2 DNA fragments were inserted respectively into NotI-EcoRI and BamHI-SalI restriction sites of pL451, to generate pL451 armed plasmid. Furthermore, 3 polyadenylation sites from pSA-Lox-Neo-tpA BamHI digested in BglII was inserted in the pL451armed. The plasmid was digested with NotI and SalI and the relevant fragment was electroporated with the plasmid pL253-P63Lox1-Ex14-3xFlag into the EL350 to generate the final construct including the recombination cassette (Fig.S3B). See Table S4 for the list of oligonucleotide primers described in this section.

Generation of the conditional knock-in L514F mutant mice

The p63L514F mutation was inserted into the p63 locus in E14TG2a (129/Ola) ES cells by homologous recombination using the recombination construct describe above linearized with NotI, essentially as previously described (1). Twenty-four hours after electroporation ES cells were selected with 100 µg/ml G418 (Thermo Fisher Scientific) for 7 days. Neo-resistant ES clones were screened at 3' and 5' for the correct insertion in the p63 endogenous locus by PCR analysis using the TaKaRa LA Taq® DNA Polymerase (Clontech) with an oligonucleotide annealing in the neomycin cassette and another on the genomic DNA (5'Arm Forward and Reverse; 3'Arm Forward and Reverse) (Figure S3C and Table S4). The homologous recombination event was also confirmed by Southern blotting (Figure S3D). Genomic DNA was digested with HindIII and analyzed with a probe located inside the neomycin cassette. An ES positive clone was injected into C57BL/6 blastocysts and the obtained chimeric mice were tested for germline transmission by breeding with C57BL/6 females. Offspring was genotyped for germline transmission of the p63L514F wild-type and mutant allele by PCR using tail genomic DNA and specific primers (L514F3xFlag For and L514F3xFlag Rev)) (Table S4). The neomycin cassette was removed by breeding the first generation of heterozygous mice with transgenic mice carrying the Flip recombinase. Mouse genotyping was performed by PCR with the indicated oligonucleotide primers (Table S4).

Protein Expression and Purification in *E. coli*

For *E. coli* expression of the murine p63 SAM L514F and subsequent structure determination by NMR, the mutant domain (amino acid 506-570) was subcloned into a pGEX-6P-2 expression vector (GE Healthcare) using the BamHI and XhoI restriction sites, and expressed in BL21(DE3)pLysS cells (Thermo Fisher Scientific). Unlabeled expression was carried out in 2xYT medium, while labeled expression was done in M9 minimal medium as described previously (8). Protein was expressed for 5hr at 23°C after induction with 1 mM IPTG, and cells were lysed by

sonification in PBS buffer supplemented with lysozyme (Sigma), DNAse (Sigma) and protease inhibitors. After centrifugation supernatant was loaded onto Glutathione Sepharose 4 Fast Flow Resin (GE Healthcare). Bound protein was washed with PBS and eluted with GST-elution buffer (50 mM Tris-HCl; 10 mM reduced glutathione; pH 8.0). Fractions containing protein were pooled and treated with Prescission-protease (GE Healthcare) for cleavage of the GST-tag. For removal of free GST and Prescission-Protease and concomitant buffer exchange cleaved protein was subjected to SEC on a Superdex 75 16/60 column (GE Healthcare) equilibrated in NMR Buffer (20 mM HEPES; 50 mM NaCl; 1 mM DTT; pH 7.0). Exchange of an unlabeled sample from H_2O to D_2O was achieved by several rounds of dilution and concentration with D_2O NMR Buffer. For concentration Amicon Centrifugal Filter Units were used (Merck Millipore).

For CD melting curve analysis of *E. coli* expressed protein, the human p63 SAM wild-type and L514F variant (amino acid 506-572) were subcloned into a pGEX-6p-2 expression vector, which was modified by substituting the PreScission-protease site with an 8xHis-tag followed by TEV-protease cleavage site, referred to as pGEX-6p-2-8xHis-TEV. The SAM domains were expressed in T7 Express cells (New England Biolabs) at 18°C overnight after induction with 1 mM IPTG. Cells were lysed by sonification in IMAC-A buffer (25 mM Tris; 200 mM NaCl; 25 mM Imidazole; pH 7.8) supplemented with lysozyme (Sigma), DNAse (Sigma) and protease inhibitors. After centrifugation the supernatant was applied on HisTrap columns (GE Healthcare). Bound protein was washed with IMAC-A buffer and eluted with IMAC-B buffer (25 mM Tris; 200 mM NaCl; 400 mM Imidazole; pH 7.8). Fractions containing protein were pooled and dialyzed in IMAC-A buffer after addition of His-tagged TEV-protease for cleavage of the GST-8xHis-tag. The cleaved tag and TEV-protease were removed by reverse IMAC purification. For final removal of impurities and concurrent exchange to CD Buffer (25mM HEPES; 100mM NaCl; 1mM DTT; pH 7.5) protein was further purified using a Superdex 75 16/60 column.

NMR Spectroscopy and structure Determination

For the backbone assignment a 3D HNCACB spectrum was used. Aliphatic and aromatic side chains were assigned with 3D [^{15}N,^{1}H]-TOCSY-HSQC, [^{15}N,^{1}H]-NOESY-HSQC (in H_2O) and 2D NOESY (in D_2O) spectra. Distance restraints were derived from [^{15}N,^{1}H]-NOESY-HSQC (in H_2O) and 2D NOESY (in D_2O) spectra.

The NMR structure of the murine p63 SAM L514F mutant was obtained using combined automated NOE assignment and structure calculation (9) with the program package CYANA (10). As input for CYANA, peak lists from [^{15}N,^{1}H]-NOESY-HSQC in H_2O and homonuclear NOESY in D_2O, the manual established chemical shift assignment, dihedral angle restraints obtained from chemical shift analysis by Talos+ (11), hydrogen bond restraints and the amino acid sequence were used. The structure calculation was performed using 200 random starting conformers and 10,000 torsion angle dynamic steps. All remaining parameters were kept at their default values. The 20 conformers with the lowest CYANA target function values were used for represent the solution structure. Restrained energy refinement was conducted using OPALp (12), which relies on the AMBER force field (13). An overview of the structural statistics is given in SI Appendix, Table S1.

Electrophoretic Mobility Shift Assay (EMSA)

After transfection with the indicated p63 wild-type or mutants expressing constructs, nuclear extracts from HEK293 cells were prepared, and EMSA was performed as described (14). Oligonucleotide primer used for EMSA correspond to the KRT14 enhancer site (14). The protein–DNA complexes

were resolved by gel electrophoresis on 5% non-denaturing polyacrylamide gels, dried and visualized by autoradiography.

SI Figures

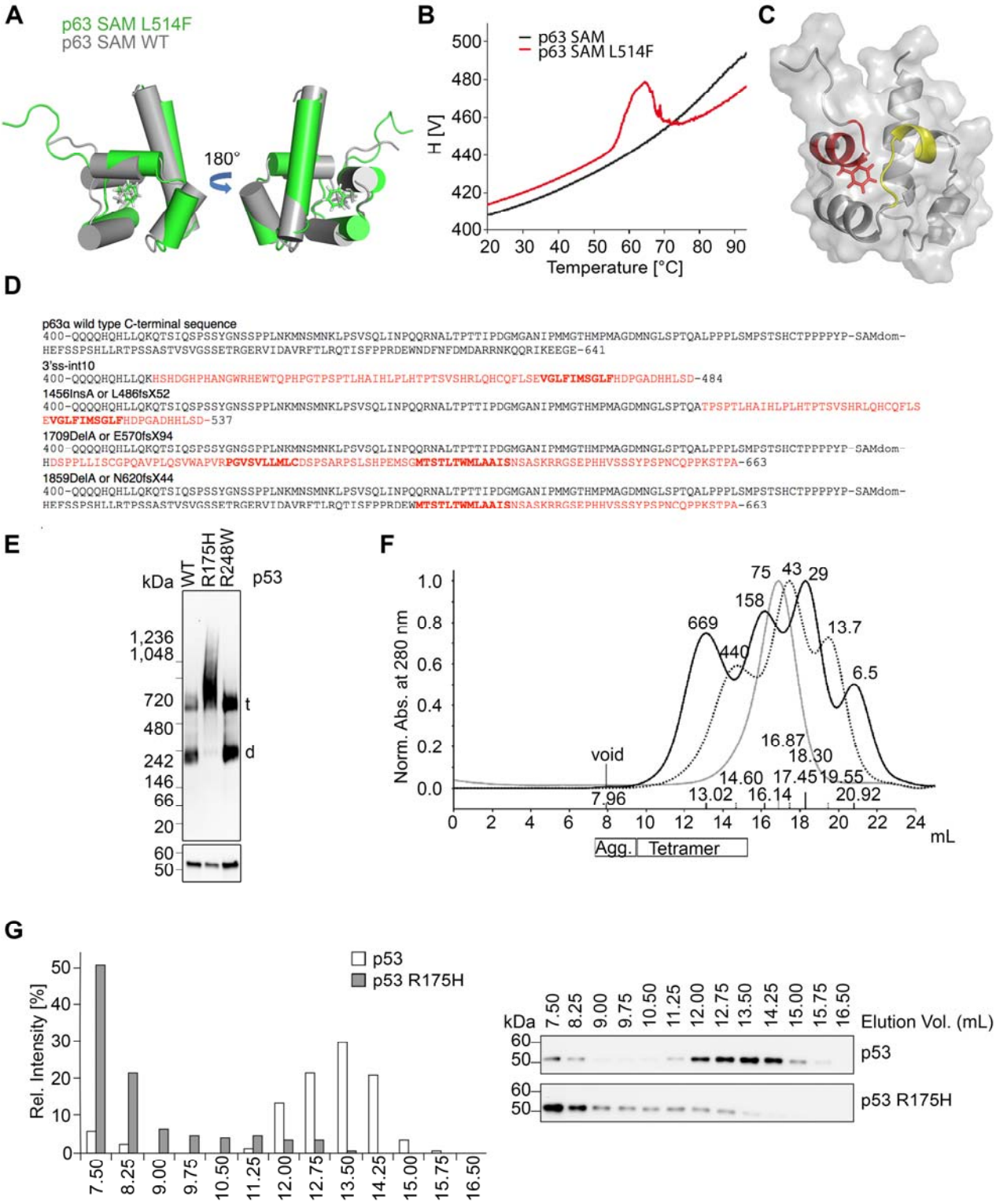

Figure S1. Aggregation propensity of mutant p63L514F

A. A representative conformer of the NMR structure of the murine p63L514F SAM (green) was superimposed with the wild type p63 SAM structure (grey; PDB: 1RG6). Amino acids L514 and F514 are depicted as sticks in their respective color.

B. Sample turbidity of wild type p63 SAM (black) and p63L514F SAM (red) as measurement of precipitation and aggregation upon unfolding during the CD melting experiment (15). Dynode voltage: H[V])

C. The two aggregation prone segments of the p63 SAM domain, a.a. 508-515 (red) and a.a. 530-537 (yellow), were mapped on the NMR structure of the L514F mutant. F514 is highlighted as sticks.
D. C-terminal sequence of wild type p63α and its frameshift mutations causative of AEC syndrome. The SAM domain sequence is indicated as -*SAMdomain*-. Amino acid generated by frameshift are indicated in red. Sequences with an aggregation propensity are indicated in bold.
E. BN-PAGE and Western blot for p53 in H1299 extracts expressing wild type p53 and two cancer mutations R175H, known to cause aggregation, and R248W that has lost the DNA binding ability. P53 run as dimer (d) and tetramer (t). SDS-PAGE as control of p53 loading is in the lower panel.
F. The Superose 6 GL 10/300 column used for SEC analysis of H1299 cell lysate was calibrated using molecular weight standards. Protein standards are expressed in kDa above the peak and the precise elution volume is on the x-axis.
G. SEC followed by Western blot of H1299 cell lysates overexpressing wild type p53 and the mutant p53R175H. Samples were incubated at 37°C for 15 min. before loading on SEC. Bar diagrams show the relative intensities of each collected fraction.

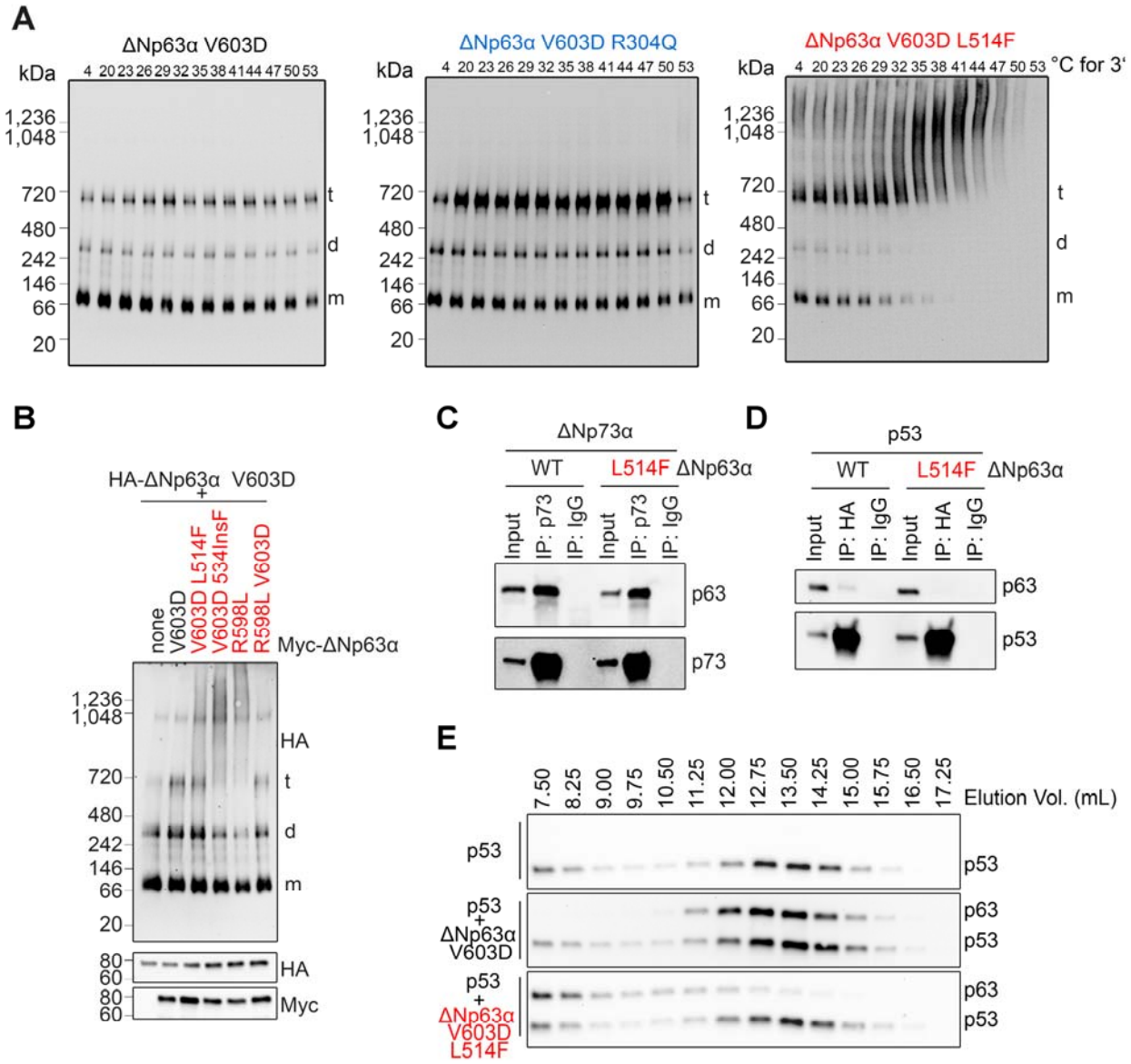

Figure S2. AEC-associated p63 mutants form aggregates with wild type p63 and others p53 family members.

A. BN-PAGE coupled with a cellular thermal shift assay (CETSA) (16) to test wild type and mutant p63 thermodynamic stability in cell lysate of H1299 cells. Soluble ΔNp63α protein ran mainly as a monomer (m) and tetramer (t) with a minor dimeric (d) population. Aggregates migrated at sizes above the tetramer.

B. BN-PAGE of co-expressed HA-tagged ΔNp63α V603D with Myc-tagged wild type or mutant p63 in H1299 cells. Immunoblot were revealed with anti-Myc or anti-Ha as indicated. SDS-PAGE as control of p63 loading is in the lower panel.

C. Co-immunoprecipitation experiment of Myc-tagged ΔNp63α wild type or L514F with ΔNp73α in H1299 cells and Western blot with the indicated antibodies.

D. Co-immunoprecipitation between wild type HA-p53 and the indicated Myc-ΔNp63α proteins. p53 was immunoprecipitated (IP) with an HA-specific antibody and detected with HA for p53, or Myc for p63.

E. SEC analysis and Western blot of p53 alone or co-expressed with ΔNp63αV603D either wild type or L514F in H1299 cells.

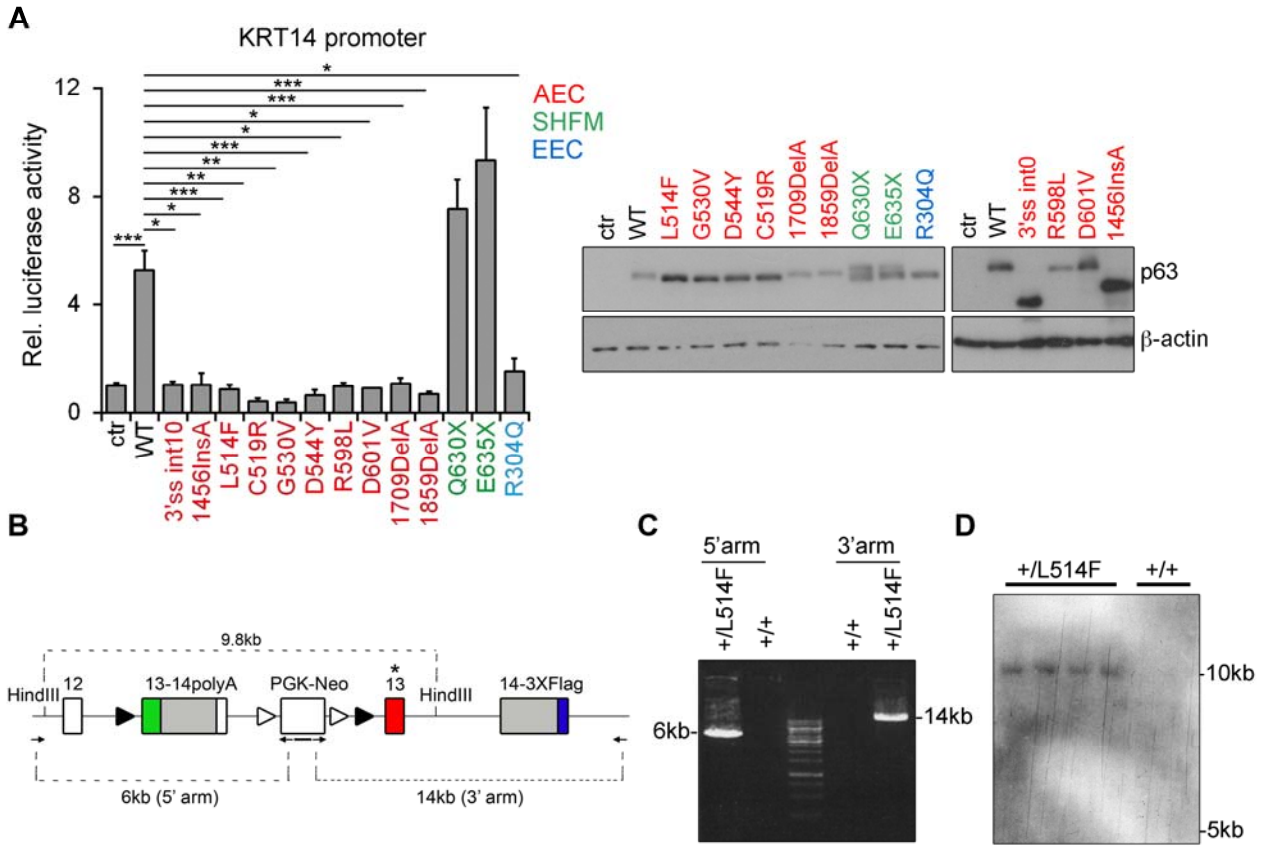

Figure S3. Transcriptional activity of wild type and mutant p63 and gene targeting strategy for the p63+/floxL514F knock-in ES cells.

A. Luciferase reporter assay (left panel) and SDS-PAGE (right panel) followed by Western blot of wild type and mutant p63 on the KRT14 promoter in HEK293 cells. β-actin was used as loading control. Data were normalized for *Renilla* luciferase activity (n=11). Data are shown as mean ± SEM and statistical significance was assessed using one-way ANOVA analysis. * $p \leq 0.05$; **; $p \leq 0.001$; ***$p \leq 0.0001$.

B. Schematic representation of the gene targeting vector used to generate the inducible p63L514F knock-in mice. The targeted locus is depicted as in Fig. 3C. The upper dotted black line indicates the fragment generated by the knock-in allele upon HindIII digestion performed in S3D. The lower dotted black lines indicate the fragments generated by PCR performed in S3C. Oligonucleotide primers (arrows, see Table S4) used for PCR analysis and the relative PCR product length are indicated.

C. PCR analysis performed on genomic DNA derived from the ES cell clone used to generate the knock-in mouse using specific oligonucleotide primers (see Table S4) in order to confirm the insertion of 5' arm and 3' arm respectively.

D. Southern blot analysis of genomic DNA derived from several ES cell clones digested with HindIII and probed with a neomycin-specific fragment (1).

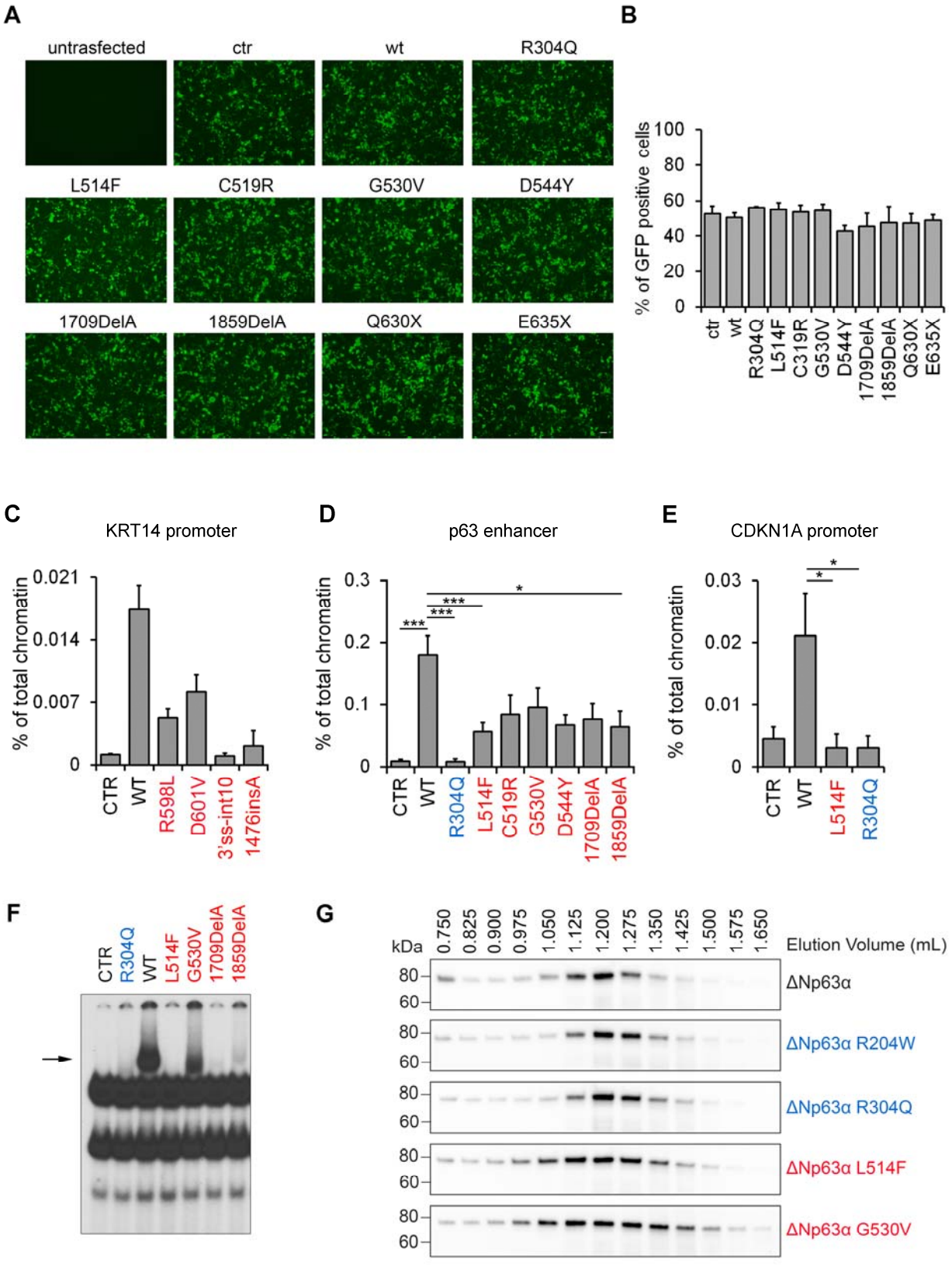

Figure S4. AEC-associated p63 mutants exhibit impaired DNA binding in cells.
A. Representative fluorescent GFP signal in HEK293 co-transfected with wild type or mutant p63 and pEGFP-C1 (Clontech) used as transfection control.
B. Quantification of GFP positive cells of the experiment in A using ImageJ software. Data are shown as mean ± SD, n=2.

C-E. ChIP-qPCR analysis in HEK293 cells overexpressing wild type and mutant p63 on the KRT14 and CDKN1A promoters (n=2, n=5 respectively), and of the p63 enhancer (n=18).
F. EMSA in HEK293 nuclear extracts of the indicated wild type and mutant p63 proteins with a radiolabeled probe corresponding to the KRT14 promoter sequence.
G. SEC analysis and Western blot of *in vitro* translated p63 proteins. Wild type and mutant p63 proteins eluted as a tetrameric protein with no signal in the aggregation fraction (0.75 ml).
Data are shown as mean ± SEM with the exception of (C) in which error bars indicate SD. Statistical significance was assessed using one-way ANOVA analysis. * $p \leq 0.05$; ***$p \leq 0.0001$.

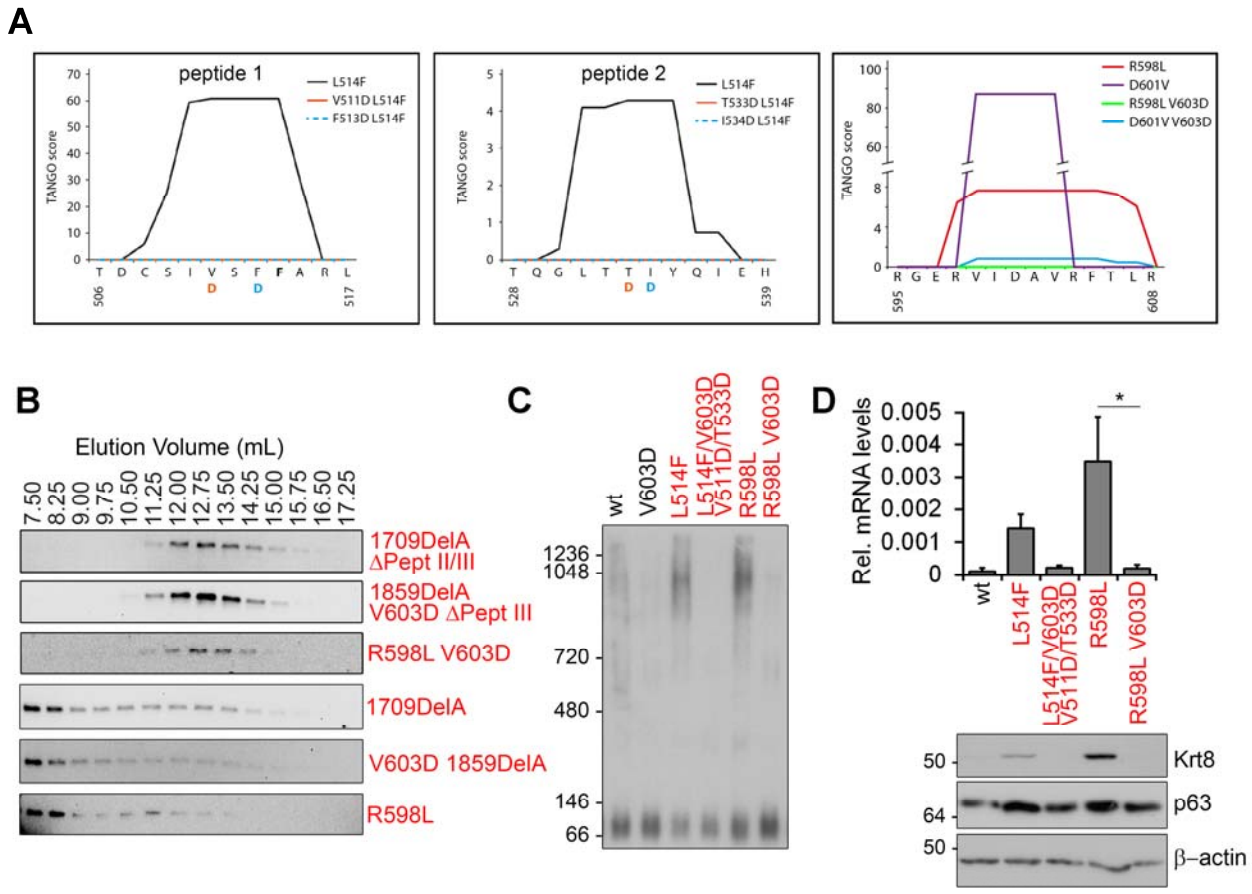

Figure S5 AEC mutant aggregation is alleviated by p63 variants predicted by TANGO

A. Graphic representation of the TANGO algorithm for the indicated p63 variants predicted to suppress aggregation of the AEC mutants. For L514F the two aggregation prone sequences in the SAM domain are shown (left and middle panel) (Table S3).

B. SEC analysis and Western blot of a selected set of rescue variants expressed in H1299 cells. All rescue mutants eluted as tetramers (fractions 11.25 to 15 ml).

C. BN-PAGE for p63 in mouse primary keratinocytes infected with retrovirus carrying wild type or mutants p63.

D. Real time RT-PCR of Krt8 (upper panel; n=4) and Western blot of Krt8 and p63 (lower panel) in mouse primary keratinocytes infected as in C. β-actin was used as loading control.

Data are shown as mean ± SEM and statistical significance was assessed using one-way ANOVA analysis. * $p \leq 0.05$.

SI TABLES

Table S1: NMR analysis of L514 mutant SAM domain. CYANA structure calculation statistics.

NOE assignment (a)	
15N-resolved NOESY-HSQC cross peaks	859
D_2O exchange NOESY cross peaks	151
Total number of NOESY cross peaks	1010
Assigned cross peaks	903 (89.4%)
Restraints	
Assigned NOE distance restraints	734 (100%)
Short range |i-j|≤1	431 (58.7%)
Medium range 1<|i-j|<5	216 (29.4%)
Long range |i-j|≥5	87 (11.9%)
Dihedral angle restraints (φ/ψ)	52
Hydrogen Bonds	46
Structure statistics (b)	
Average CYANA target function value ($Å^2$)	1.82±0.35
Average AMBER Energies (kcal/mol)	-2498±46
Restraint violations (c)	
Max. distance restraint violation (Å)	0.0
Number of violated distance restraints > 0.2 Å	0
Max. dihedral angle restraint violations (°)	6.42
Number of violated dihedral angle constraints > 5°	1
Ramachandran plot	
Residues in most favoured regions	87.2%
Residues in additionally allowed regions	11.8%
Residues in generously allowed regions	1.0%
Residues in disallowed regions	0.0%
RMSD (residues 9-69)	
Average backbone RMSD to mean (Å)	0.43±0.10
Average heavy atom RMSD to mean (Å)	0.92±0.10

(**a**) using automated NOE assignment and structure calculation functionalities of CYANA
(**b**) after restrained energy minimization with OPALp
(**c**) after energy minimization, calculated with CYANA

Table S2: β-aggregation propensity of the p63 C-terminal domain and mutants predicted by the TANGO algorithm

AEC point mutations are highlighted in bold.

	WT		L514F		G530V		D544Y	
residue number	residue	TANGO score	residue	TANGO score	residue	TANGO score	residue	TANGO score
506	T	0	T	0	T	0	T	0
507	D	0	D	0	D	0	D	0
508	C	3.893	C	5.845	C	3.857	C	3.852
509	S	16.807	S	24.985	S	16.641	S	16.621
510	I	39.745	I	59.269	I	39.275	I	39.231
511	V	40.727	V	60.736	V	40.244	V	40.199
512	S	40.727	S	60.736	S	40.244	S	40.199
513	F	40.727	F	60.736	F	40.244	F	40.199
514	L	40.448	**F**	60.547	L	39.965	L	39.921
515	A	19.002	A	28.463	A	18.781	A	18.759
516	R	0	R	0	R	0	R	0
517	L	0	L	0	L	0	L	0
518	G	0	G	0	G	0	G	0
519	C	0	C	0	C	0	C	0
520	S	0	S	0	S	0	S	0
521	S	0	S	0	S	0	S	0
522	C	0	C	0	C	0	C	0
523	L	0	L	0	L	0	L	0
524	D	0	D	0	D	0	D	0
525	Y	0	Y	0	Y	7.575	Y	0
526	F	0	F	0	F	9.646	F	0
527	T	0	T	0	T	9.908	T	0
528	T	0	T	0	T	10.485	T	0
529	Q	0	Q	0	Q	11.602	Q	0
530	G	0.296	G	0.293	**V**	42.921	G	0.293
531	L	4.136	L	4.097	L	45.118	L	4.089
532	T	4.136	T	4.097	T	44.618	T	4.089
533	T	4.321	T	4.281	T	44.496	T	4.272
534	I	4.321	I	4.281	I	44.364	I	4.272
535	Y	4.321	Y	4.281	Y	36.161	Y	4.272
536	Q	0.731	Q	0.727	Q	5.452	Q	0.725
537	I	0.731	I	0.727	I	5.104	I	0.725
538	E	0	E	0	E	0	E	0
539	H	0	H	0	H	0	H	0
540	Y	0	Y	0	Y	0	Y	0
541	S	0	S	0	S	0	S	0
542	M	0	M	0	M	0	M	0
543	D	0	D	0	D	0	D	0
544	D	0	D	0	D	0	**Y**	1.085
545	L	0	L	0	L	0	L	1.085
546	A	0	A	0	A	0	A	1.085

547	S	0	S	0	S	0	S	1.085
548	L	0	L	0	L	0	L	1.085
549	K	0	K	0	K	0	K	0
550	I	0	I	0	I	0	I	0
551	P	0	P	0	P	0	P	0
552	E	0	E	0	E	0	E	0
553	Q	0	Q	0	Q	0	Q	0
554	F	0	F	0	F	0	F	0
555	R	0	R	0	R	0	R	0
556	H	0	H	0	H	0	H	0
557	A	0	A	0	A	0	A	0
558	I	0	I	0	I	0	I	0
559	W	0	W	0	W	0	W	0
560	K	0	K	0	K	0	K	0
561	G	0	G	0	G	0	G	0
562	I	0	I	0	I	0	I	0
563	L	0	L	0	L	0	L	0
564	D	0	D	0	D	0	D	0
565	H	0	H	0	H	0	H	0
566	R	0	R	0	R	0	R	0
567	Q	0	Q	0	Q	0	Q	0
568	L	0	L	0	L	0	L	0
569	H	0	H	0	H	0	H	0
570	E	0	E	0	E	0	E	0
571	F	0	F	0	F	0	F	0
572	S	0	S	0	S	0	S	0

	WT		**1456 InsA (AEC)**		**1572 InsA (EEC)**		**1743 DelAA (EEC)**		**1709 DelA (AEC)**		**1859 DelA (AEC)**	
residue number	**residue**	**TANGO score**	**residue**	**TANGO score**	**residue**	**TANGO score**	**residue**	**TANGO score**	**residue**	**TANGO score**	**residue**	**TANGO score**
480	L	0	L	0	L	0	L	0	L	0	L	0
481	S	0	S	0	S	0	S	0	S	0	S	0
482	P	0	P	0	P	0	P	0	P	0	P	0
483	T	0	T	0	T	0	T	0	T	0	T	0
484	Q	0	Q	0	Q	0	Q	0	Q	0	Q	0
485	A	0	A	0	A	0	A	0	A	0	A	0
486	L	0	**T**	0	L	0	L	0	L	0	L	0
487	P	0	P	0	P	0	P	0	P	0	P	0
488	P	0	S	0	P	0	P	0	P	0	P	0
489	P	0	P	0	P	0	P	0	P	0	P	0
490	L	0	T	0	L	0	L	0	L	0	L	0
491	S	0	L	0	S	0	S	0	S	0	S	0
492	M	0	H	0	M	0	M	0	M	0	M	0
493	P	0	A	0	P	0	P	0	P	0	P	0
494	S	0	I	0	S	0	S	0	S	0	S	0
495	T	0	H	0	T	0	T	0	T	0	T	0
496	S	0	L	0	S	0	S	0	S	0	S	0
497	H	0	P	0	H	0	H	0	H	0	H	0

498	C	0	L	0	C	0	C	0	C	0	C	0
499	T	0	H	0	T	0	T	0	T	0	T	0
500	P	0	T	0	P	0	P	0	P	0	P	0
501	P	0	P	0	P	0	P	0	P	0	P	0
502	P	0	T	0	P	0	P	0	P	0	P	0
503	P	0	S	0	P	0	P	0	P	0	P	0
504	Y	0	V	0	Y	0	Y	0	Y	0	Y	0
505	P	0	S	0	P	0	P	0	P	0	P	0
506	T	0	H	0	T	0	T	0	T	0	T	0
507	D	0	R	0	D	0	D	0	D	0	D	0
508	C	3.893	L	0	C	3.789	C	3.797	C	3.792	C	3.812
509	S	16.807	Q	0	S	16.356	S	16.391	S	16.369	S	16.457
510	I	39.745	H	0	I	38.624	I	38.803	I	38.727	I	38.935
511	V	40.727	C	0	V	39.577	V	39.762	V	39.685	V	39.898
512	S	40.727	Q	0	S	39.577	S	39.762	S	39.685	S	39.898
513	F	40.727	F	0	F	39.577	F	39.762	F	39.685	F	39.898
514	L	40.448	L	0	L	39.305	L	39.49	L	39.413	L	39.625
515	A	19.002	S	0	A	18.464	A	18.552	A	18.515	A	18.614
516	R	0	E	0	R	0	R	0	R	0	R	0
517	L	0	V	23.371	L	0	L	0	L	0	L	0
518	G	0	G	24.559	G	0	G	0	G	0	G	0
519	C	0	L	34.323	C	0	C	0	C	0	C	0
520	S	0	F	35.7	S	0	S	0	S	0	S	0
521	S	0	I	35.801	S	0	S	0	S	0	S	0
522	C	0	M	26.495	C	0	C	0	C	0	C	0
523	L	0	S	16.056	L	0	L	0	L	0	L	0
524	D	0	G	12.223	**E**	0	D	0	D	0	D	0
525	Y	0	L	11.888	L	0	Y	0	Y	0	Y	0
526	F	0	F	9.96	F	0	F	0	F	0	F	0
527	T	0	H	0	H	0	T	0	T	0	T	0
528	T	0	D	0	D	0	T	0	T	0	T	0
529	Q	0	P	0	P	0	Q	0	Q	0	Q	0
530	G	0.296	G	0	G	0	G	0.285	G	0.284	G	0.286
531	L	4.136	A	0	A	0	L	3.982	L	3.969	L	4.003
532	T	4.136	D	0	D	0	T	3.982	T	3.969	T	4.003
533	T	4.321	H	0	H	0	T	4.16	T	4.146	T	4.182
534	I	4.321	H	0	H	0	I	4.16	I	4.146	I	4.182
535	Y	4.321	L	0	L	0	Y	4.16	Y	4.146	Y	4.182
536	Q	0.731	S	0	S	0	Q	0.703	Q	0.701	Q	0.707
537	I	0.731	D	0	D	0	I	0.703	I	0.701	I	0.707
538	E	0					E	0	E	0	E	0
539	H	0					H	0	H	0	H	0
540	Y	0					Y	0	Y	0	Y	0
541	S	0					S	0	S	0	S	0
542	M	0					M	0	M	0	M	0
543	D	0					D	0	D	0	D	0
544	D	0					D	0	D	0	D	0
545	L	0					L	0	L	0	L	0
546	A	0					A	0	A	0	A	0
547	S	0					S	0	S	0	S	0
548	L	0					L	0	L	0	L	0
549	K	0					K	0	K	0	K	0

550	I	0					I	0	I	0	I	0
551	P	0					P	0	P	0	P	0
552	E	0					E	0	E	0	E	0
553	Q	0					Q	0	Q	0	Q	0
554	F	0					F	0	F	0	F	0
555	R	0					R	0	R	0	R	0
556	H	0					H	0	H	0	H	0
557	A	0					A	0	A	0	A	0
558	I	0					I	0	I	0	I	0
559	W	0					W	0	W	0	W	0
560	K	0					K	0	K	0	K	0
561	G	0					G	0	G	0	G	0
562	I	0					I	0	I	0	I	0
563	L	0					L	0	L	0	L	0
564	D	0					D	0	D	0	D	0
565	H	0					H	0	H	0	H	0
566	R	0					R	0	R	0	R	0
567	Q	0					Q	0	Q	0	Q	0
568	L	0					L	0	L	0	L	0
569	H	0					H	0	H	0	H	0
570	E	0					E	0	**D**	0	E	0
571	F	0					F	0	S	0	F	0
572	S	0					S	0	P	0	S	0
573	S	0					S	0	P	0	S	0
574	P	0					P	0	L	0.52	P	0
575	S	0					S	0	L	0.52	S	0
576	H	0					H	0	I	0.52	H	0
577	L	0					L	0	S	0.52	L	0
578	L	0					L	0	C	0.52	L	0
579	R	0					R	0	G	0	R	0
580	T	0					T	0	P	0	T	0
581	P	0					P	0	Q	0	P	0
582	S	0					**Q**	0	A	0	S	0
583	S	0					C	0	V	0	S	0
584	A	0					L	0	P	0	A	0
585	S	0					Y	0	L	0	S	0
586	T	0					S	0	Q	0	T	0
587	V	0					Q	0	S	0	V	0
588	S	0					C	0	V	0	S	0
589	V	0					G	0	W	0	V	0
590	G	0					L	0	A	0	G	0
591	S	0					Q	0	P	0	S	0
592	S	0							V	0	S	0
593	E	0							R	0	E	0
594	T	0							P	0.088	T	0
595	R	0							G	10.371	R	0
596	G	0							V	47.019	G	0
597	E	0							S	49.615	E	0
598	R	0							V	65.539	R	0
599	V	0.867							L	65.87	V	0.837
600	I	0.867							L	65.811	I	0.837
601	D	0.867							M	58.206	D	0.837

602	A	0.867							L	49.885	A	0.837
603	V	0.867							C	11.908	V	0.837
604	R	0.867							D	0	R	0.837
605	F	0.867							S	0	F	0.837
606	T	0.497							P	0	T	0.479
607	L	0.497							S	0	L	0.479
608	R	0							A	0	R	0
609	Q	0							R	0	Q	0
610	T	0							P	0	T	0
611	I	0							S	0	I	0
612	S	0							L	0	S	0
613	F	0							S	0	F	0
614	P	0							H	0	P	0
615	P	0							P	0	P	0
616	R	0							E	0	R	0
617	D	0							M	0	D	0
618	E	0							S	0	E	0
619	W	0							G	0	W	0.442
620	N	0							M	0.553	**M**	0.694
621	D	0							T	1.091	T	1.234
622	F	0							S	2.448	S	2.598
623	N	0							T	13.776	T	13.969
624	F	0							L	32.82	L	33.083
625	D	0							T	36.223	T	36.499
626	M	0							W	41.541	W	41.837
627	D	0							M	42.797	M	43.097
628	A	0							L	42.722	L	43.021
629	R	0							A	39.749	A	40.037
630	R	0							A	36.95	A	37.228
631	N	0							I	34.167	I	34.435
632	K	0							S	3.695	S	3.709
633	Q	0							N	0	N	0
634	Q	0							S	0	S	0
635	R	0							A	0	A	0
636	I	0							S	0	S	0
637	K	0							K	0	K	0
638	E	0							R	0	R	0
639	E	0							R	0	R	0
640	G	0							G	0	G	0
641	E	0							S	0	S	0
642									E	0	E	0
643									P	0	P	0
644									H	0	H	0
645									H	0	H	0
646									V	0	V	0
647									S	0	S	0
648									S	0	S	0
649									S	0	S	0
650									Y	0	Y	0
651									P	0	P	0
652									S	0	S	0
653									P	0	P	0

654									N	0	N	0
655									C	0	C	0
656									Q	0	Q	0
657									P	0	P	0
658									P	0	P	0
659									K	0	K	0
660									S	0	S	0
661									T	0	T	0
662									P	0	P	0
663									A	0	A	0

	WT		V603D		R598L		D601V		R598L V603D		D601V V603D	
residue number	residue	TANGO score	residue	TANGO score	residue	TANGO score	residue	TANGO score	residue	TANGO score	residue	TANGO score
594	T	0	T	0	T	0	T	0	T	0	T	0
595	R	0	R	0	R	0	R	0	R	0	R	0
596	G	0	G	0	G	0	G	0	G	0	G	0
597	E	0	E	0	E	0	E	0	E	0	E	0
598	R	0	R	0	**L**	6.443	R	0	**L**	0	R	0
599	V	0.854	V	0	V	7.648	V	87.234	V	0	V	0.825
600	I	0.854	I	0	I	7.648	I	87.234	I	0	I	0.825
601	D	0.854	D	0	D	7.648	**V**	87.234	D	0	**V**	0.825
602	A	0.854	A	0	A	7.648	A	87.234	A	0	A	0.825
603	V	0.854	<u>D</u>	0	V	7.648	V	87.234	<u>D</u>	0	<u>D</u>	0.825
604	R	0.854	R	0	R	7.648	R	0	R	0	R	0.825
605	F	0.854	F	0	F	7.648	F	0	F	0	F	0.825
606	T	0.489	T	0	T	7.293	T	0	T	0	T	0.474
607	L	0.489	L	0	L	6.091	L	0	L	0	L	0.474
608	R	0	R	0	R	0	R	0	R	0	R	0
609	Q	0	Q	0	Q	0	Q	0	Q	0	Q	0
610	T	0	T	0	T	0	T	0	T	0	T	0
611	I	0	I	0	I	0	I	0	I	0	I	0
612	S	0	S	0	S	0	S	0	S	0	S	0
613	F	0	F	0	F	0	F	0	F	0	F	0
614	P	0	P	0	P	0	P	0	P	0	P	0
615	P	0	P	0	P	0	P	0	P	0	P	0
616	R	0	R	0	R	0	R	0	R	0	R	0

Table S3: β-aggregation propensity of the p63L514F and its rescue variants predicted by the TANGO algorithm

The L514F point mutation is highlighted in bold, while the suppression mutations are underlined.

	WT	L514F	L514F V511D	L514F F513D	L514F T533D	L514F I534D

residue number	residue	TANGO score	residue	TANGO score	residue	TANGO score	residue	TANGO score	residue	TANGO score	residue	TANGO score
506	T	0	T	0	T	0	T	0	T	0	T	0
507	D	0	D	0	D	0	D	0	D	0	D	0
508	C	3.893	C	5.845	C	0	C	0	C	5.859	C	5.859
509	S	16.807	S	24.985	S	0	S	0	S	25.046	S	25.046
510	I	39.745	I	59.269	I	0	I	0	I	59.369	I	59.369
511	V	40.727	V	60.736	D	0	V	0	V	60.837	V	60.837
512	S	40.727	S	60.736	S	0	S	0	S	60.837	S	60.837
513	F	40.727	F	60.736	F	0	D	0	F	60.837	F	60.837
514	L	40.448	**F**	60.547	**F**	0	**F**	0	**F**	60.649	**F**	60.649
515	A	19.002	A	28.463	A	0	A	0	A	28.511	A	28.511
516	R	0	R	0	R	0	R	0	R	0	R	0
517	L	0	L	0	L	0	L	0	L	0	L	0
518	G	0	G	0	G	0	G	0	G	0	G	0
519	C	0	C	0	C	0	C	0	C	0	C	0
520	S	0	S	0	S	0	S	0	S	0	S	0
521	S	0	S	0	S	0	S	0	S	0	S	0
522	C	0	C	0	C	0	C	0	C	0	C	0
523	L	0	L	0	L	0	L	0	L	0	L	0
524	D	0	D	0	D	0	D	0	D	0	D	0
525	Y	0	Y	0	Y	0	Y	0	Y	0	Y	0
526	F	0	F	0	F	0	F	0	F	0	F	0
527	T	0	T	0	T	0	T	0	T	0	T	0
528	T	0	T	0	T	0	T	0	T	0	T	0
529	Q	0	Q	0	Q	0	Q	0	Q	0	Q	0
530	G	0.296	G	0.293	G	0.294	G	0.294	G	0	G	0
531	L	4.136	L	4.097	L	4.111	L	4.111	L	0	L	0
532	T	4.136	T	4.097	T	4.111	T	4.111	T	0	T	0
533	T	4.321	T	4.281	T	4.295	T	4.295	D	0	T	0
534	I	4.321	I	4.281	I	4.295	I	4.295	I	0	D	0
535	Y	4.321	Y	4.281	Y	4.295	Y	4.295	Y	0	Y	0
536	Q	0.731	Q	0.727	Q	0.729	Q	0.729	Q	0	Q	0
537	I	0.731	I	0.727	I	0.729	I	0.729	I	0	I	0
538	E	0	E	0	E	0	E	0	E	0	E	0
539	H	0	H	0	H	0	H	0	H	0	H	0
540	Y	0	Y	0	Y	0	Y	0	Y	0	Y	0
541	S	0	S	0	S	0	S	0	S	0	S	0
542	M	0	M	0	M	0	M	0	M	0	M	0
543	D	0	D	0	D	0	D	0	D	0	D	0
544	D	0	D	0	D	0	D	0	D	0	D	0
545	L	0	L	0	L	0	L	0	L	0	L	0
546	A	0	A	0	A	0	A	0	A	0	A	0
547	S	0	S	0	S	0	S	0	S	0	S	0
548	L	0	L	0	L	0	L	0	L	0	L	0
549	K	0	K	0	K	0	K	0	K	0	K	0
550	I	0	I	0	I	0	I	0	I	0	I	0
551	P	0	P	0	P	0	P	0	P	0	P	0
552	E	0	E	0	E	0	E	0	E	0	E	0
553	Q	0	Q	0	Q	0	Q	0	Q	0	Q	0

554	F	0	F	0	F	0	F	0	F	0	F	0
555	R	0	R	0	R	0	R	0	R	0	R	0
556	H	0	H	0	H	0	H	0	H	0	H	0
557	A	0	A	0	A	0	A	0	A	0	A	0
558	I	0	I	0	I	0	I	0	I	0	I	0
559	W	0	W	0	W	0	W	0	W	0	W	0
560	K	0	K	0	K	0	K	0	K	0	K	0
561	G	0	G	0	G	0	G	0	G	0	G	0
562	I	0	I	0	I	0	I	0	I	0	I	0
563	L	0	L	0	L	0	L	0	L	0	L	0
564	D	0	D	0	D	0	D	0	D	0	D	0
565	H	0	H	0	H	0	H	0	H	0	H	0
566	R	0	R	0	R	0	R	0	R	0	R	0
567	Q	0	Q	0	Q	0	Q	0	Q	0	Q	0
568	L	0	L	0	L	0	L	0	L	0	L	0
569	H	0	H	0	H	0	H	0	H	0	H	0
570	E	0	E	0	E	0	E	0	E	0	E	0
571	F	0	F	0	F	0	F	0	F	0	F	0
572	S	0	S	0	S	0	S	0	S	0	S	0

Table S4: List of oligonucleotide primers used in this study

Oligonucleotide primers for mutagenesis and cloning.		
Mutation	**Forward 5'-3'**	**Reverse 5'-3'**
E639X	CAGCGCATCAAAGAGTAGGGGGAGTGAGCC	GGCTCACTCCCCCTACTCTTTGATGCGCTG
Q634X	CGCCGCAATAAGCAATAGCGCATCAAAGAGGAG	CTCCTCTTTGATGCGCTATTGCTTATTGCGGCG
1709DelA94	CCGGCAGCTCCACGATTCTCCTCCCCTTCT	AGAAGGGGAGGAGAATCGTGGAGCTGCCGG
1859DelA	CCCCGAGATGAGTGGATGACTTCAACTTTGACATGG	CCATGTCAAAGTTGAAGTCATCCACTCATCTCGGGG
1709DelA (cloning)	CCCGGCGGCCGCGTTGTACCTGGAAAACAATGCCC	AGATCATCCATGGAGTAATGCTC
1859DelA (cloning)	GAGCATTACTCCATGGATGATCT	GCGGAGATCTTCCCCTAAGAAATCAGACAAGAGG
pBABE-DNp63a (cloning)	CCCGGGATCCCTCGTTTAGTGAACCGTCAGAATTG	CCGGATCCTCATTCTCCTTCCTCTTTGATACGCTG
p63L514F V511D	CGTATCCCACAGATTGCAGCATTGATAGTTTCTTTGCGAGGTTGGGCTGTTC	GAACAGCCCAACCTCGCAAAGAAACTATCAATGCTGCAATCTGTGGGATACG
p63L514F F513D	CCACAGATTGCAGCATTGTCAGTGATTTTGCGAGGTTGGGCTGTTC	GAACAGCCCAACCTCGCAAAATCACTGACAATGCTGCAATCTGTGG
p63T533D	CGACCCAGGGGCTGACCGATATCTATCAGATTGAGCATTACTCC	GGAGTAATGCTCAATCTGATAGATATCGGTCAGCCCCTGGGTCG

p63I534D	CCAGGGGCTGACCACCGATTATCAGATTGAGCATTACTCCATG	CATGGAGTAATGCTCAATCTGATAATCGGTGGTCAGCCCCTGG
p631709DelA ΔPept II	CTCCAGTGAGACCCGGGGATTCACCCTCCGCCAGAC	GTCTGGCGGAGGGTGAATCCCCGGGTCTCACTGGAG
p631709DelA ΔPept III	GAGATGAGTGGAATGACTTCAACTAGCAACAGCGCATCAAAGAGG	CCTCTTTGATGCGCTGTTGCTAGTTGAAGTCATTCCACTCATCTC
p631859DelA ΔPept III	GAGATGAGTGGATGACTTCAACTAGCAACAGCGCATCAAAGAGG	CCTCTTTGATGCGCTGTTGCTAGTTGAAGTCATCCACTCATCTC
p633'ss-int10/1456InsA ΔPept I	CAGCATTGTCAGTTTCTTAGCGAGCACGACCCAGGGGCTG	CAGCCCCTGGGTCGTGCTCGCTAAGAAACTGACAATGCTG
p63R598L V603D	GTGAGACCCGGGGTGAGCTGGTTATTGATGCTGACCGATTCACC	GGTGAATCGGTCAGCATCAATAACCAGCTCACCCCGGGTCTCAC
p63D601V V603D	CCCGGGGTGAGCGTGTTATTGTGGCTGACCGATTCACCCTCCGCCAG	CTGGCGGAGGGTGAATCGGTCAGCCACAATAACACGCTCACCCCGGG
Oligonucleotide primers for Real Time RT-PCR		
Gene	**Forward 5'-3'**	**Reverse 5'-3'**
mTrp63 ex12-13 wt	ACTCTCCATGCCCTCCAC	GAGCAGCCCAACCTTGCT
mTrp63 ex12-13 L514F	ACTCTCCATGCCCTCCAC	GAGCAGCCCAACCTTGCA
mActb	CTAAGGCCAACCGTGAAAAGAT	GCCTGGATGGCTACGTACATG
mKrt5	CAACGTCAAGAAGCAGTGTGC	TTGCTCAGCTTCAGCAATGG
mKrt14	GATGTGACCTCCACCAACCG	CCATCGTGCACATCCATGAC
mDsc3	CCACCGTCTCTCACTACATGGA	TGTCCTGAACTTTCATTATCAGTTTGT
mIrf6	CAGCTCTCTCCCCATGACTGA	CCCATACTCCTTCCCACGATAC
mFgfr2	TGGATCGAATTCTGACTCTCACA	TTCGAGAGGCTGGGTGAGAT
mSmad7	AACGAGAGTCAGCACTGCCA	GAAGGTGGTGCCCACTTTCA
mCdkn1a	GAACATCTCAGGGCCGAAAA	CAATCTGCGCTTGGAGTGAT
mKrt8	TGCTCATGTTCTGCATCCCA	GATCACCACCTACCGCAAGC
hKRT14	GGATGACTTCCGCACCAAGT	TCCACACTCATGCGCAGGT
hIRF6	CAGCTCTCTCCCCATGACTGA	CCCATACTCCTTCCCACGATAC
hDSC3	CCACCGTCTCTCACTACATGGA	TGTCCTGAACTTTCATTATCAGTTTGT
Oligonucleotide primers for ChIP-qPCR.		
p63 binding site	**Forward 5'-3'**	**Reverse 5'-3'**

human P63 enhancer	CGTTCCAAAGCCTAACCTGATCA	TTTTCCCAAACTCCAACCTG
human FGFR2 enhancer	CCCCGTGGCCGAAAA	GAAAGCGCAGGCGAGTTCT
human KRT14 promoter	GGGCCTGTCTGAGGAGATAGG	AGGCATGTTGAGAGGAATGTGA
human CDKN1A promoter	TTCAAGGCAGTGGGAGAAGG	TGGTTGTCAAATGTCCAGCAG
mouse p63 enhancer	CTGCGTGTGCGTTGCATATAA	CGTCATGTCTCCCTGCCTTC
mouse Irf6 enhancer	AGCCTCCCAGTTACAAGTAGCAA	TGCCACCACTTTCCCAGTCT
mouse Fgfr2 enhancer	GGGCGCCTGATTGCTTT	CAGCCTGGACTCATTTTCATCTG
mouse Smad7 promoter	GTGAGGCGAAAGAAGAGCCC	GCTCTGACTGGCTTGTATGCC
mouse Krt8 enhancer	GCCATACCCAGGCATCCATA	CACACAACACCCACTACCCCT
Oligonucleotide primers for the generation of the conditional knock-in construct.		
Ap63CDNU	ATTAGCGGCCGCGTAGAGGAGCCAAAATTTGCTGAC	
Ap63CDNL	GCCGAAGCTTGCACTGCCTTCTATCCCCACAC	
Bp63CDNU	GCCGAAGCTTCAATCATAAGAGCTCTTAACATCAC	
Bp63CDNL	GCCGACTAGTTGAGCACAGATTCCTCTGTGGGAC	
CmP63U	ATTAGCGGCCGCCAGAGGCACATGTAGCCCCACAG	
CmP63L	GCCGGAATTCTTGGGGGGTCTCTTAGGATGTTTCA	
DmP63U	ATTAGGATCCGCACAAAATAGCCAATATAGT	
DmP63L	ATTAGTCGACGCTGAGGTCCAAGGAGTGCTCC	
C1P63U	ATTAGCGGCCGCATGCAGGAAACTCAATCCCCA	
C1P63L	GCCGGAATTCAGTTAAATGAGAAGGCAAAAGTCTC	
D1P63U	ATTAGGATCCGCGCCCATTGCGGGGTTCTTCC	
D1P63L	GCCGGTCGACTTAGACTATAAGGCTGAAAATGC	
P63ex14fgU	GTTACAAACTTCAAGGCCTGTTAGC	
P63ex14fgL	TAATCCCGGGCTTCTCCTTCCTCTTTGATACGCTG	
ISceIE14U	GCCGAGTTACGCTAGGGATAACAGGGTAATATAGGCCGTCTGCACTATTTTACACA	
ICeuIFlagL	GCCGTTCGCTACCTTAGGACCGTTATAGTTACGGGATCACTACTTGTCATCGTC	
DmP63U2	ATTAGCGGCCGCGCACAAAATAGCCAATATAGT	
Ex13L2	GCTCAATCTGATAGATGGTGGTC	

Ex13U2	GACCACCATCTATCAGATTGAGC	
RecEx14L3	ATTAGAATTCAGATCTCATTCTCCTTCCTCTTTGATACGC	
DmP63U	ATTAGGATCCGCACAAAATAGCCAATATAGT	
Ex13MutL	CCCAACCTTGCAAAGAAACTGC	
Ex13mutU	GCAGTTTCTTTGCAAGGTTGGG	
RecEx13L	ATTAGTCGACTTTTTAACCAATCTCTGAGTAAG	
Oligonucleotide primers for Screening PCR of ES cells.		
name	**Forward 5'-3'**	**Reverse 5'-3'**
5'Arm	TATAGTCCCAGTGCTGCAAGTGCT	GATCCCATGGTTTAGTTCCTCACC
3'Arm	ATGGCTTCTGAGGCGGAAAGAACCAG	AAGCCCCATGAAATGACACGACAGAAT
Oligonucleotide primers for mouse genotyping.		
L514F3xFlag For	CAGCGTATCAAAGAGGAAGGAGA	
L514F3xFlag Rev	AGCCAGAATCAGAATCAGGTGAC	

Table S5: List of antibodies used in this study

Antibodies		
rabbit polyclonal anti-p63 (H137)	Santa Cruz Biotechnology	Cat#sc-8343
mouse monoclonal anti-p63 (4A4)	Santa Cruz Biotechnology	Cat#sc-8431
rabbit anti-Keratin 14	Covance	Cat#PRB-155P
mouse monoclonal anti-ß-Actin (AC-15)	Santa Cruz Biotechnology	Cat#sc-69879
rabbit anti-IRF6	Ferone et al., 2012 (1)	N/A
mouse monoclonal anti-p73	Millipore	Cat# OP109L
goat polyclonal anti-HA	Bethyl Laboratories	Cat# A190-138A
rabbit polyclonal anti-ERK1 (K-23)	Santa Cruz Biotechnology	Cat# sc-94
mouse monoclonal anti-Myc (4A6)	Millipore	Cat# 05-724
normal mouse IgG	Santa Cruz Biotechnology	Cat# sc-2025
normal rabbit IgG	Santa Cruz Biotechnology	Cat# sc-2027
sheep anti-mouse IgG HRP	GE Healthcare	Cat# NA931
donkey anti-rabbit IgG HRP	GE Healthcare	Cat# NA934

References

1. Ferone G*, et al.* (2012) Mutant p63 causes defective expansion of ectodermal progenitor cells and impaired FGF signalling in AEC syndrome. *EMBO molecular medicine* 4(3):192-205.
2. Candi E*, et al.* (2006) Differential roles of p63 isoforms in epidermal development: selective genetic complementation in p63 null mice. *Cell death and differentiation* 13(6):1037-1047.
3. Kern SE*, et al.* (1992) Oncogenic forms of p53 inhibit p53-regulated gene expression. *Science* 256(5058):827-830.
4. Antonini D*, et al.* (2015) A composite enhancer regulates p63 gene expression in epidermal morphogenesis and in keratinocyte differentiation by multiple mechanisms. *Nucleic acids research* 43(2):862-874.
5. Takahashi K & Yamanaka S (2006) Induction of pluripotent stem cells from mouse embryonic and adult fibroblast cultures by defined factors. *Cell* 126(4):663-676.
6. Chen Y, Mistry DS, & Sen GL (2014) Highly rapid and efficient conversion of human fibroblasts to keratinocyte-like cells. *The Journal of investigative dermatology* 134(2):335-344.
7. Liu P, Jenkins NA, & Copeland NG (2003) A highly efficient recombineering-based method for generating conditional knockout mutations. *Genome research* 13(3):476-484.
8. Gebel J*, et al.* (2016) Mechanism of TAp73 inhibition by DeltaNp63 and structural basis of p63/p73 hetero-tetramerization. *Cell death and differentiation* 23(12):1930-1940.
9. Guntert P & Buchner L (2015) Combined automated NOE assignment and structure calculation with CYANA. *Journal of biomolecular NMR* 62(4):453-471.
10. Guntert P, Mumenthaler C, & Wuthrich K (1997) Torsion angle dynamics for NMR structure calculation with the new program DYANA. *Journal of molecular biology* 273(1):283-298.
11. Shen Y, Delaglio F, Cornilescu G, & Bax A (2009) TALOS+: a hybrid method for predicting protein backbone torsion angles from NMR chemical shifts. *Journal of biomolecular NMR* 44(4):213-223.
12. Koradi R, Billeter M, & Guntert P (2000) Point-centered domain decomposition for parallel molecular dynamics simulation. *Comput Phys Commun* 124(2-3):139-147.
13. Ponder JW & Case DA (2003) Force fields for protein simulations. *Advances in protein chemistry* 66:27-85.
14. Romano RA, Birkaya B, & Sinha S (2007) A functional enhancer of keratin14 is a direct transcriptional target of deltaNp63. *The Journal of investigative dermatology* 127(5):1175-1186.
15. Benjwal S, Verma S, Rohm KH, & Gursky O (2006) Monitoring protein aggregation during thermal unfolding in circular dichroism experiments. *Protein science : a publication of the Protein Society* 15(3):635-639.
16. Martinez Molina D*, et al.* (2013) Monitoring drug target engagement in cells and tissues using the cellular thermal shift assay. *Science* 341(6141):84-87.